

# A two-body femtoscopy approach to the proton-deuteron correlation function

Juan M. Torres-Rincon<sup>1</sup>, Àngels Ramos<sup>1</sup>, Joel Ruff<sup>2</sup>

<sup>1</sup>*Departament de Física Quàntica i Astrofísica, Facultat de Física, Universitat de Barcelona, Martí i Franquès 1, 08028 Barcelona, Spain and Institut de Ciències del Cosmos (ICCUB),*

*Facultat de Física, Universitat de Barcelona, Martí i Franquès 1, 08028 Barcelona, Spain and*

<sup>2</sup>*Facultat de Física, Universitat de Barcelona, Martí i Franquès 1, 08028 Barcelona, Spain*

(Dated: November 1, 2024)

The proton-deuteron correlation function measured by the ALICE collaboration in high multiplicity p+p collisions shows a momentum dependence which is in contradiction with the predictions of the Lednický-Lyuboshitz formalism of the two-body interaction. This result motivated a more sophisticated three-body description in terms of a composed deuteron. Encouraged by the good description of other deuteron observables in the context of heavy-ion collisions we revisit this correlation function under the two-body approximation not relying on the Lednický-Lyuboshitz approximation, but using the solution of the Schrödinger equation incorporating both strong and Coulomb interactions. The two-body description provides a reasonable agreement to ALICE data for natural values of the source size. Interpreting the previously assumed attractive character of the  $(L, S) = (0, 3/2)$  channel of the  $pd$  interaction into a more-likely repulsion, the results agree better not only with the ALICE measurements but also with recent STAR data in Au+Au collisions.

## I. INTRODUCTION

Femtoscopy has emerged as a powerful technique in relativistic heavy-ion collisions (RHICs) to gain information of the system spacetime properties as well as details from hadron interactions [1–6]. For a recent review on this field see Ref. [7]. Accessing the details of particle interactions is most appealing for systems in which scattering experiments cannot be performed. Typical examples are particles that decay fast due to weak interactions and stable beams cannot be conceived. Femtoscopy of hyperons and other heavy particles with strangeness or charm have already been analyzed at the HADES experiment at GSI [8], STAR experiment at BNL [9, 10], and ALICE experiment at LHC [11–27].

Femtoscopy of nuclei has also become possible in which deuteron or more massive states have been addressed. Recently, femtoscopy studies considering proton and deuteron pairs have been performed in high-multiplicity p+p collisions at  $\sqrt{s} = 13$  TeV by the ALICE [28] experiment, in Au+Au collisions at  $\sqrt{s_{NN}} = 3$  GeV measured by the STAR experiment [29], and in Ag+Ag collisions at  $\sqrt{s_{NN}} = 2.55$  GeV by the HADES experiment [30].

In the case of p+p collisions produced at the LHC [28] the  $pd$  correlation function has been compared by ALICE with the theoretical prediction provided by the so-called Lednický-Lyuboshitz (LL) approximation [31, 32], which uses the two-body  $L = 0$  wave function in its asymptotic form, taking the low-energy scattering parameters (scattering length and scattering range) as the only inputs. These parameters were fixed from the experimental scattering data of Ref. [33]. As it can be seen in [28] this approximation completely fails in describing the experimental correlation function providing totally opposed quantitative results. In the LL approximation the strong interaction dominates over the Coulomb barrier due to the large values of the scattering length (specially in the very attractive  ${}^4S_{3/2}$  channel). On the contrary, the experimental data show a small strong modification to the repulsive electromagnetic interaction.

Following these results, it was advocated in Ref. [34] that a full three-body description of the  $pd$  scattering problem was needed. This would account for the intrinsic structure of the deuteron, and a more complex formalism was developed for this goal. The final result—also incorporating higher partial waves than  $L = 0$ —shows a very good agreement with data [28], arriving to the conclusion that accounting for the internal structure of the deuteron is essential to describe the  $pd$  system.

While the size of the deuteron is comparable to the typical range of the emitting source, the use of a point like deuteron in RHIC studies has brought results that are consistent with experimental data in several sectors [35]: yields and spectra [36, 37], elliptic flow [36, 38], etc. Also the freeze-out multiplicities are successfully predicted by the statistical thermal model [39, 40], where the deuteron is modelled on equal footing as the rest of hadrons. For this reason one would expect that the low-energy description of the  $pd$  system with a elementary deuteron should be still possible as a first approximation to the real physics. We believe that before discarding the two-body approach in favor of a three-body formalism (without diminishing the value of that approach) one needs to (in)validate the two-body description by addressing it beyond the LL approximation.

In this paper we revisit the proton-deuteron problem solving the Schrödinger equation with strong and Coulomb interactions and compute the full wave function valid in all space, and not only in the asymptotic region. In the standard application of the LL approach, it only considers low-energy scattering parameters in the  $L = 0$  partial wave. In our current approach, we are not

limited by the low-energy expansion of the scattering amplitude and produce higher partial waves beyond the  $S$  wave.

## II. PROTON-DEUTERON INTERACTION: WOODS-SAXON AND GAUSSIAN POTENTIALS

We start by setting the two-body interaction potentials between a proton and a deuteron using experimental information from the phase shifts at low energies. We will use data in different spin ( $S$ ) and angular momentum ( $L$ ) channels from Ref. [33].

To access the wave function in a given channel we solve the quantum two-body problem using a potential in position space  $V(r)$  by means of the Schrödinger equation,

$$-\frac{\hbar^2}{2\mu}\nabla^2\psi(\mathbf{r}) + V(r)\psi(\mathbf{r}) = E\psi(\mathbf{r}) , \quad (1)$$

where  $\mu$  is the reduced mass of the  $pd$  system and  $E = \hbar^2k^2/(2\mu)$  is the total energy of the system in the center of mass frame. We analyze the solution of (1) by looking for bound states ( $E < 0$ ) as well as for scattering states, which we eventually use in the correlation function (see Sec. III).

We use two sets of phenomenological potentials. The first one is taken from Ref. [41], and has a Woods-Saxon (WS) form,

$$V_{\text{WS}}(r) = \frac{V_0}{1 + e^{(r-R)/a}} , \quad (2)$$

where  $V_0$ ,  $a$ , and  $R$  are parameters that depend on  $S$  and  $L$ . The total spin of the  $pd$  pair can be  $S = \{1/2, 3/2\}$ , while we will take orbital angular momentum values up to  $L = 2$ , which is the maximum partial wave analyzed in Ref. [33].

The parameters in Eq. (2) are given of Ref. [41], and were calculated from fits to the scattering data in [33]. There is a total of 18 parameters (3 for each spin-orbit channel) which we reproduce for convenience in Table I. In this table we also quote the values of the binding energies that we obtain for the bound states—without incorporating Coulomb interaction—that appear in different channels. Apart from the state with  $S = 1/2$ , which could be identified with the  ${}^3\text{He}$  nucleus, there is another bound state with smaller binding energy in the  $S = 3/2$  channel, which cannot be associated to any known physical state as  ${}^3\text{He}$  has no known nuclear excitations.

In the case of states in the continuum, we turn on the Coulomb potential and solve the Schrödinger equation as a function of the relative momentum  $k$ ,

$$\left( \frac{d^2}{dr^2} + k^2 - U(r) - \frac{L(L+1)}{r^2} \right) u_L(r, k) = 0 , \quad (3)$$

	$S = 1/2$			$S = 3/2$		
	$L = 0$	$L = 1$	$L = 2$	$L = 0$	$L = 1$	$L = 2$
$V_0$ (MeV)	-29.754	-8.214	-7.849	-18.115	-13.10	14.878
$R$ (fm)	2.826	2.962	2.974	2.837	2.067	2.527
$a$ (fm)	1.187	0.259	0.991	0.9655	1.578	1.235
$E_B$ (MeV)	-7.780			-2.539		

TABLE I. Values of the potential depth ( $V_0$ ), the size ( $R$ ), and the surface thickness parameter ( $a$ ) of the Woods-Saxon potential (2) for the proton-deuteron interaction, taken from Ref. [41]. They are fitted to reproduce the experimental  $pd$  scattering phase shifts in [33]. Bottom row: binding energies of the bound states found by solving the Schrödinger equation in the different ( $S, L$ ) channels.

where  $U(r) = 2\mu[V(r) + \alpha/r]$ ,  $\alpha$  is the fine structure constant, and  $L$  is the orbital angular momentum. We solve the equation for  $u_L(r)$  using the Numerov algorithm [42], and the solution in the outer region of the potential is matched to the asymptotic form [43, 44],

$$u_L(r, k) = k^{-1} e^{i\Delta_L} \left[ \cos \hat{\delta}_L F_L(\gamma; kr) - \sin \hat{\delta}_L G_L(\gamma; kr) \right], \quad (4)$$

where  $\gamma = \mu\alpha/k$ ,  $F_L(\gamma; kr)$  and  $G_L(\gamma; kr)$  are the regular and irregular Coulomb wave functions, respectively. These are incorporated in our code using the subroutines of Ref. [45]. Finally,  $\Delta_L = \sigma_L + \hat{\delta}_L$  is a global phase shift that contains the Coulomb phase shift,  $\sigma_L = \arg \Gamma(1 + L + i\gamma)$ , and an additional phase shift,  $\hat{\delta}_L$ , that incorporates the effect of the strong interaction (but not equal to the pure strong phase shift [44]).

The resulting phase shifts  $\hat{\delta}_L$  (with Coulomb effects) using the WS potentials are compared in Fig. 1 (dotted blue lines) to the experimental data extracted from [33] as functions of the kinetic energy of the incident proton in the laboratory frame,  $T_p = E(m_p + m_d)/m_d$ , with  $m_p$  and  $m_d$  the proton and deuteron mass, respectively.

From Fig. 1 we observe a general good agreement of the results using the WS potential given in [41] and the experimental phase shifts, with sizable deviations in the  $S = 1/2, L = 1$  and  $S = 3/2, L = 2$  cases. It is important to notice that in the  $S = 3/2, L = 0$  channel the phase shift starts at  $\pi$  and decreases, signature of the bound state found in that channel (see Table I). However, the existence of such a state is dubious, and the attractive nature of this channel can be questioned due to the ambiguity of  $\pi$  in the extraction of the scattering phase shifts.

For this reason we try an alternative parametrization of the same experimental phase shifts but reinterpret the  $S = 3/2, L = 0$  channel. On one hand we would like to use a simple form of the

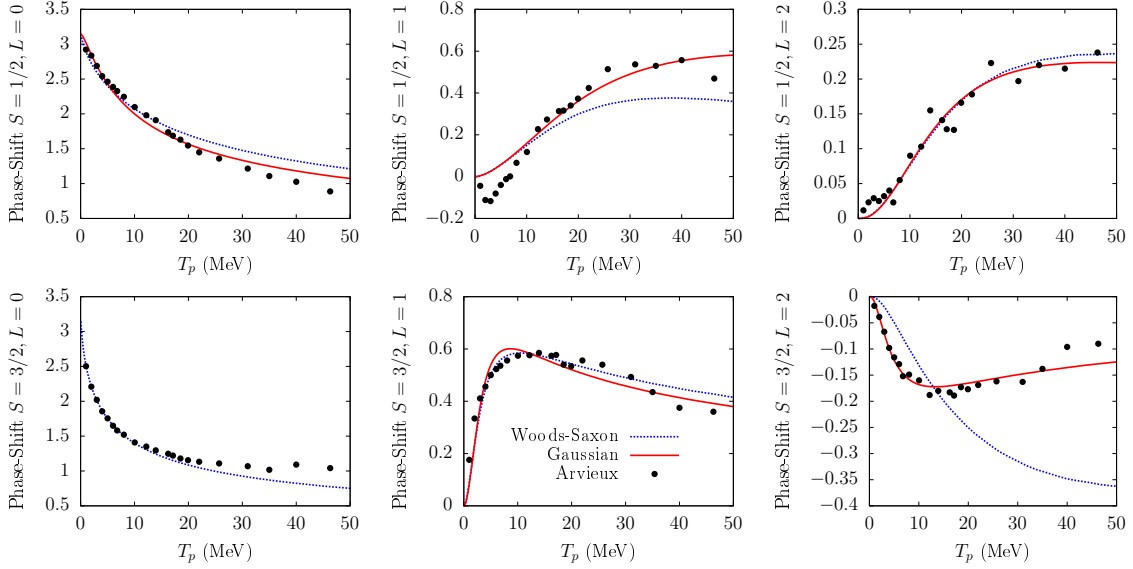


FIG. 1. Results of the calculated  $pd$  scattering phase shifts using the WS (dotted blue lines) and Gaussian (solid red lines) potentials, together with the experimental results from Ref. [33]. The Gaussian fit to the  $S = 3/2, L = 0$  phase-shift is shown in Fig. 2.

potentials with a lesser number of parameters than the WS parametrization. Therefore, we use a Gaussian form,

$$V_{\text{Gauss}}(r) = \bar{V}_0 \exp\left(-\frac{r^2}{r_G^2}\right), \quad (5)$$

where the potential strength  $\bar{V}_0$  and the potential range  $r_G$  are parameters depending on  $S$  and  $L$ .

On the other hand, we reanalyze the  $S = 3/2, L = 0$  channel and consider it to be repulsive due to the absence of any physical bound state with  $J = 3/2$ . Then we shift down the quoted  ${}^4S_{3/2}$  phase shift in [33] by  $\pi$  in all its energy domain. This interpretation is consistent with the  $S = 3/2, L = 0$  phase shifts considered in several references [46–49] which start at zero and decrease with energy, showing a pure repulsive interaction.

We perform fits of the experimental phase shifts in Ref. [33] using the potential (5) for each channel using the MINUIT package to generate the best fit parameters. The resulting fitting parameters of the Gaussian potentials are shown in Table II. In this table we also provide the binding energy of the obtained bound state in the  $S = 1/2, L = 0$  channels (without the Coulomb force). We find the state identified with the  ${}^3\text{He}$  to have a similar binding energy compared to that in the WS case. As expected, we find no bound state in the repulsive channel  $S = 3/2, L = 0$ .

The resulting phase shifts obtained in the fit of Gaussian potentials are shown in Fig. 1 in solid red lines. Using a lesser number of parameters (12 vs 18) we are able to obtain satisfactory fits

	$S = 1/2$			$S = 3/2$		
	$L = 0$	$L = 1$	$L = 2$	$L = 0$	$L = 1$	$L = 2$
$\bar{V}_0$ (MeV)	-15.7	-49.0	-7.4	28.8	-6.8	1.4
$r_G$ (fm)	$5.3 \pm 0.3$	$1.7 \pm 0.3$	$3.5 \pm 0.2$	$3.9 \pm 0.2$	$4.5 \pm 0.3$	$7.4 \pm 1.2$
$E_B$ (MeV)	-7.87					

TABLE II. Parameters of the  $pd$  Gaussian potential of Eq. (5) obtained by fitting experimental phase shifts of [33] for the considered  $S, L$  channels. Bottom row: Binding energy of the bound state found in the  $S = 1/2, L = 0$  channel.

and even improve the description of the  $S = 1/2, L = 1$  and  $S = 3/2, L = 2$  channels, as compared to the WS case.

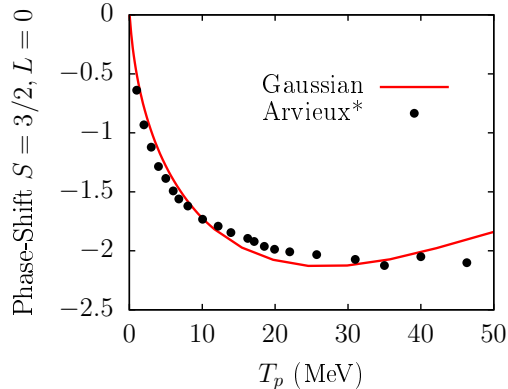


FIG. 2. Phase shifts of the  $pd$  scattering in the  $S = 3/2, L = 0$  channel using the Gaussian potential in Eq. (5). Symbols are the experimental result of [33] for this channel, but incorporating a down shift of  $\pi$ —due to the  $\pi$ -ambiguity of the phase-shift—to reinterpret the result as a repulsive interaction [46].

The  $S = 3/2, L = 0$  phase shifts calculated with the Gaussian potential are plotted in the separate Fig. 2. We superimpose the experimental data from Ref. [33] shifted down a value of  $\pi$  (denoted as Arvieux\*) to match the results with the repulsive interaction described in Ref. [46]. The fit is rather good and provides a repulsive potential which, as we said, admits no bound state as opposed to the WS case.

### III. PROTON-DEUTERON CORRELATION FUNCTION

Once we obtain the  $pd$  wave functions for any value of  $k$  as a function of  $r$ , we can address the femtoscopy correlation function. To compute it we use the Koonin-Pratt equation [1, 50],

$$C(k) = \int S(\mathbf{r}) |\Phi(\mathbf{r}; \mathbf{k})|^2 d^3r , \quad (6)$$

where  $S(\mathbf{r})$  is the source function depending on the relative distance of the pair and  $\Phi(\mathbf{r}; \mathbf{k})$  is the two-body wave function in the CM frame. For the source function we choose a normalized Gaussian profile that depends only on the relative distance  $r$  [7],

$$S(\mathbf{r}) = (4\pi r_0^2)^{-3/2} \exp\left(-\frac{r^2}{4r_0^2}\right) , \quad (7)$$

where  $r_0$  is the radius parameter that defines the typical distance between a proton and a deuteron at freeze-out. In our calculations this quantity is estimated using experimental conditions (depending on the colliding system, collision centrality, etc.) or used as a free parameter.

The total wave function includes both strong and Coulomb interactions and it can be rewritten in the following convenient form using a partial wave sum,

$$\Phi(r, z; k) = \Phi^C(r, z; k) + \sum_L (2L+1) [\Phi_L(r; k) - \Phi_L^C(kr)] P_L(\cos\theta) , \quad (8)$$

where  $z = r \cos\theta$ , and  $\theta$  the relative angle between  $\mathbf{r}$  and  $\mathbf{k}$ . In Eq. (8) the complete Coulomb wave function is given by [44],

$$\Phi^C(r, z; k) = e^{-\pi\gamma/2} \Gamma(1+i\gamma) e^{ikz} {}_1F_1(-i\gamma; 1; ik(r-z)) , \quad (9)$$

with  $\Gamma(a)$  being the Euler's gamma function and  ${}_1F_1(a, b; c)$  the confluent hypergeometrical function or Kummer's function. The  $L$  partial-wave of the Coulomb wave function is given by [44],

$$\Phi_L^C(kr) = (kr)^{-1} i^L e^{i\sigma_L} F_L(\gamma; kr) . \quad (10)$$

Inserting the square of (8) into the correlation function, and using that the source is spherically symmetric one gets,

$$C(k) = \int S(r) |\Phi^C(r, z; k)|^2 d^3r + \int 4\pi r^2 S(r) \sum_{L=0}^{L_{\max}} (2L+1) \left[ \left| \frac{u_L(r, k)}{r} \right|^2 - |\Phi_L^C(kr)|^2 \right] dr , \quad (11)$$

where  $u_L(r, k)$  is the reduced radial wave function with angular momentum  $L$ , computed by the method detailed in the preceding section. Notice that we have truncated the partial wave sum up to a maximum value  $L_{\max}$  assuming that the sum converges.

We present the results for the correlation function adding one by one the different partial waves, using a fixed value of the source radius,  $r_0$ , and performing the averaging over the  $S = 1/2$  and  $S = 3/2$  spins,

$$C(k) = \frac{{}^2C(k) + 2{}^4C(k)}{3}. \quad (12)$$

The results are shown in Fig. 3. In the left column we present the results using the WS potentials and in the right column the results of the Gaussian potentials. For the top panels we use a small radius of  $r_0 = 1.0$  fm typical from p+p collisions, while in the bottom panels we use  $r_0 = 3$  fm, more consistent with mid peripheral heavy-ion collisions.

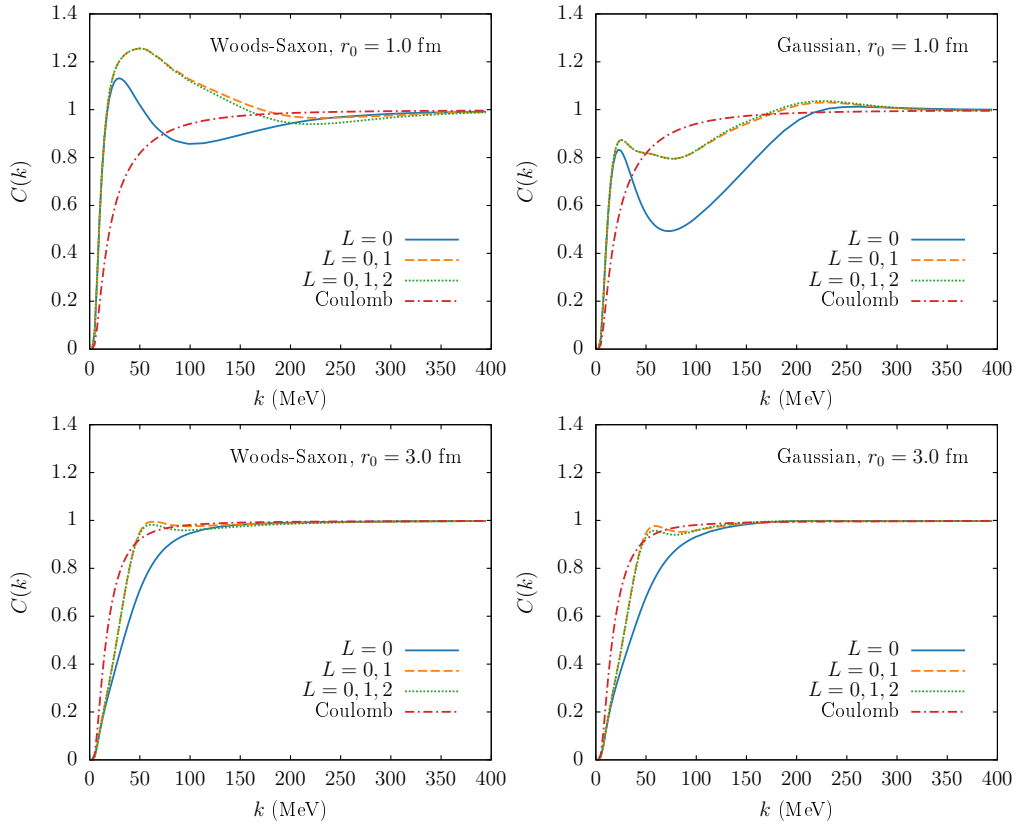


FIG. 3.  $pd$  correlation function for the WS (left column) and Gaussian potential (right column), obtained by adding successive partial waves  $L = 0, 1, 2$ . Top row: Source radius of  $r_0 = 1$  fm. Bottom row:  $r_0 = 3$  fm.

The dotted-dashed red line is the result of using the Coulomb interaction only. It serves as a baseline that reflects the electromagnetic repulsion of the pair, signalled by the correlation function lower than unity [7]. The solid blue, dashed orange and dotted green lines are the results adding the strong interaction up to partial waves  $L^{\max} = 0, 1, 2$ , respectively.



We observe that the main effect comes from the  $L = 0$  wave, which presents a bound state in the  $S = 1/2$  channel. In addition, the WS case also admits a bound state in the  $S = 3/2, L = 0$  channel. The effect of adding the  $L = 1$  partial wave is important for both models, producing a visible increase around  $k = 100$  MeV. The effect of the  $L = 2$  partial wave is very small in both models and for both Gaussian radii, showing a fast convergence of the partial wave expansion.

We have seen that different potentials produce variations in the wave functions for the same  $(S, L)$  close to  $r = 0$ . In turn, this effect produces differences in the correlation function. With larger values of the source size  $r_0$ , the part of the wave function that contributes more to the correlation function is shifted toward the asymptotic region. Since the potentials are fitted with information of that precise region i.e. the phase shifts, then the resulting correlation functions are alike (except for the different phase shifts of the  $S = 3/2, L = 0$  channel, as commented). In fact, the LL approximation should work better for larger radii, since the relevant part of the wave function becomes closer to the asymptotic part.

After discussing the effect of the sequential addition of partial waves we present the results with  $L_{\max} = 2$  as a function of the potential used (WS versus Gaussian) and the source radius,  $r_0$ . In the left column of Fig. 4 we present the results using the WS potentials (with a strongly attractive  ${}^4S_{3/2}$  channel), while in the right column we show the results using the Gaussian potential (with a repulsive  ${}^4S_{3/2}$  channel). In the top panels we focus of  $pd$  correlation functions with small source radii  $r_0 = 1, 1.5, 2$  fm, relevant for small systems, like those produced in high-multiplicity p+p collisions at the LHC. We superimpose the experimental results from the ALICE collaboration for this system [28]. With a source size of  $r_0 = 1.0$  fm we observe a prominent peak in the WS model that cannot describe the data, while the Gaussian potential with the same source radius improves the description significantly. Sources with  $r_0 = 1.5, 2$  fm can roughly describe data in both models, but these radii are slightly larger than the effective source radius quoted by the ALICE collaboration in [28]. In any case, our results demonstrate that the two-body description beyond the LL approximation—that is, solving the whole wave function via the Schrödinger equation—makes a satisfying job.

In the bottom panel we use larger source radii,  $r_0 = 2, 3, 4$  fm, relevant for larger collision systems. We superimpose data from mid peripheral Au+Au collisions as measured by STAR collaboration from BNL [29] (we do not incorporate errors bars, since they are difficult to extract from the figures as they are very small). Our results overpredict the data points, especially in the WS model, possibly due to the extra attraction caused by the  ${}^4S_{3/2}$  bound state. For the Gaussian potential (top, left panel) the agreement improves a bit, thus favouring the repulsive

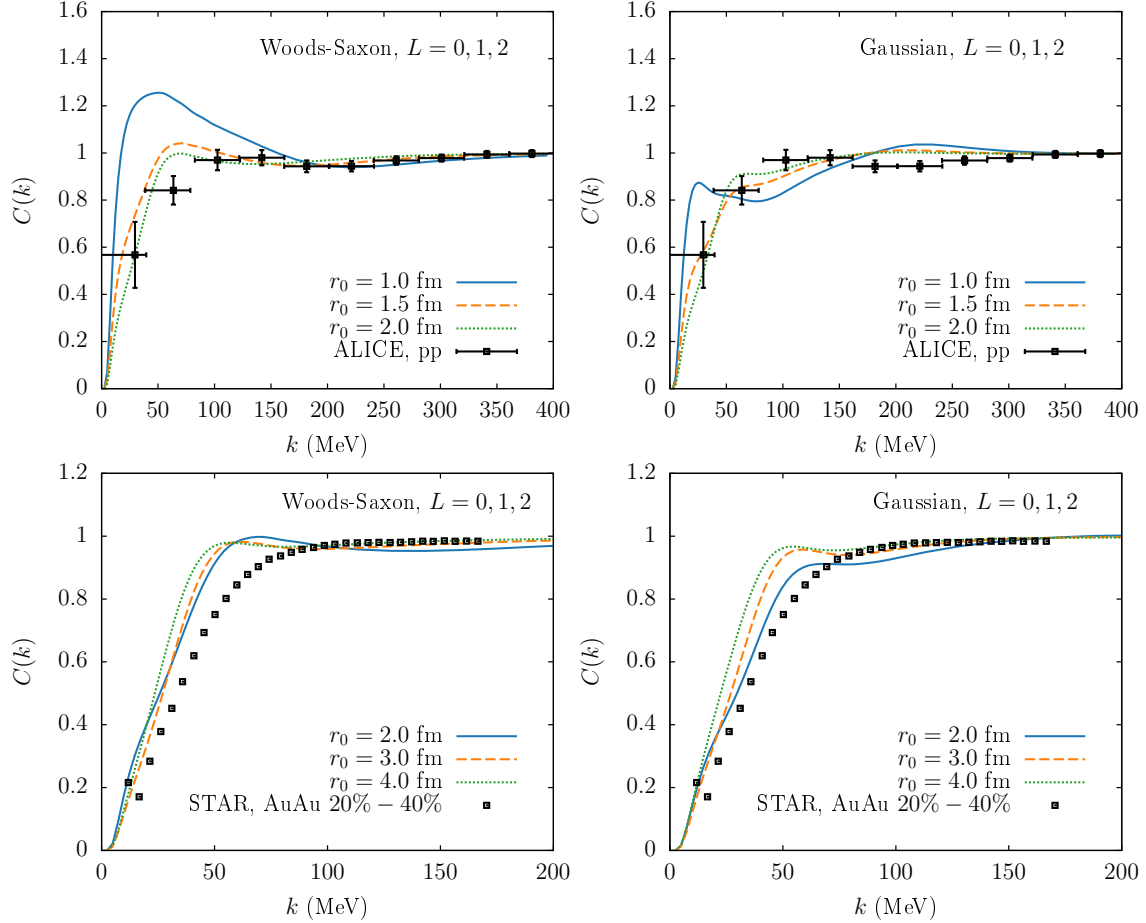


FIG. 4. Left column:  $pd$  correlation function including  $L = 0, 1, 2$  partial waves using the WS potentials, for different values of the Gaussian radius. Right column: Same as left column but using the Gaussian potentials for the  $pd$  scattering. We superimposed experimental data from ALICE [27] and STAR [29] collaborations.

$^4S_{3/2}$  interaction, but overpredicting the data for a source radius similar to that quoted by STAR collaboration,  $r_0 \simeq 3$  fm [29].

We again observe that a two-body potential between the proton and the deuteron provides a reasonable description of the  $pd$  correlation function. While a three-body interaction model [34] results in a more complete and seemingly more precise description of the ALICE data [28], the simplicity of a two-body problem makes such an approach worthwhile. The claimed failure of the two-body description by Ref. [28] is most likely due to the LL approximation used, and not because of a genuine insufficiency of the two-body description, as we have just seen.

#### IV. CONCLUSIONS

In this work we have studied the  $pd$  system and its femtoscopy under the assumption of a two-body interacting potential. We have calculated the femtoscopy correlation function with source radii relevant for p+p as well as for heavy-ion collisions. To analyze the  $pd$  interaction we have considered two sets of potentials for the  $S = \{1/2, 3/2\}$  and  $L = \{0, 1, 2\}$  channels. We have first used Woods-Saxon potentials obtained in [41] using experimental phase shift data from [33]. The fitted potentials present a bound state in the  $S = 1/2, L = 0$  channel—the  ${}^3\text{He}$ —as well as an unidentified bound state in the  $S = 3/2, L = 0$  channel. Alternatively, we have fitted Gaussian potentials for the very same channels, but reinterpreting the  ${}^4S_{3/2}$  phase shift in [33] as a repulsive interaction, as done in previous works [46–49]. We have obtained better fits to the phase shifts with a lesser number of parameters.

The resulting wave functions obtained from the Schrödinger equation have been used to predict the  $pd$  correlation function for the two models as functions of the radius  $r_0$  of a Gaussian source. Overall, we have found a good theoretical description for the experimental data in both p+p and Au+Au collisions using two-body dynamics. While a three-body problem like the one proposed in Ref. [34] might result on a better approximation to the problem, we find a reasonably good agreement with a much simpler technology. In previous works [28, 34], the two-body description was claimed to completely fail for the description of the experimental data. However, the correlation function was calculated not using the complete wave function, but applying the LL approximation [32], which takes into account only the asymptotic form of the wave function (in general, only valid for large sources). We have shown here employing two-body dynamics only, but going beyond this approximation leads to a reasonable description of the data. These results should then be considered as a realistic two-body benchmark that can of course be improved by sophisticated three-body treatment as that of Ref. [27, 34].

#### V. NOTE ADDED

After the completion of this work and during the writing of the manuscript, the preprint [51] appeared. The motivation and the methodology of this papers coincides with the ones here, and the results are entirely compatible with ours. We fully agree with the conclusions of [51] noting that the Lednický-Lyuboshitz approximation might not be reliable for small sources and, in particular, for correlation functions involving the deuteron.

The potential used in [51] is a combination of square wells, while here we have used Woods-Saxon and a Gaussian profiles. For comparison, we present in Fig. 5 the  $pd$  correlation function with a source radius of  $r_0 = 3$  fm taken from [51] together with our calculations with the WS and Gaussian potentials. All calculations are taken up to  $L = 2$ . We observe small differences tied to the particular form of the potentials that provide a different behavior of the wave functions for  $r \lesssim 3$  fm.

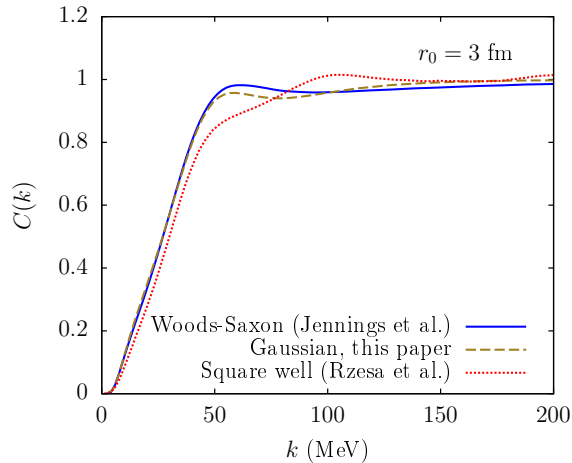


FIG. 5. Comparison of the  $pd$  correlation function from the solution of the 2-body Schrödinger equation with different potentials, the Woods-Saxon potential from [41], the Gaussian potential parametrized in this work, and a combination of squares wells from the recent Ref. [51].

#### ACKNOWLEDGMENTS

We thank Scott Pratt for an enlightening discussion after the appearance of Ref. [51] on the important role of the  ${}^4S_{3/2}$  channel in the  $pd$  scattering.

This work has been supported by the project number CEX2019-000918-M (Unidad de Excelencia “María de Maeztu”), PID2020-118758GB-I00 and PID2023-147112NB-C21, financed by the Spanish MCIN/ AEI/10.13039/501100011033/. JMT-R also thanks the Deutsche Forschungsgemeinschaft (DFG) through the CRC-TR 211 “Strong- interaction matter under extreme conditions” for support.

---

[1] S. E. Koonin, Phys. Lett. B **70**, 43 (1977).

[2] W. Bauer, C. K. Gelbke, and S. Pratt, Ann. Rev. Nucl. Part. Sci. **42**, 77 (1992).

- [3] G. Baym, *Acta Phys. Polon. B* **29**, 1839 (1998), arXiv:nucl-th/9804026.
- [4] U. A. Wiedemann and U. W. Heinz, *Phys. Rept.* **319**, 145 (1999), arXiv:nucl-th/9901094.
- [5] U. W. Heinz and B. V. Jacak, *Ann. Rev. Nucl. Part. Sci.* **49**, 529 (1999), arXiv:nucl-th/9902020.
- [6] M. A. Lisa, S. Pratt, R. Soltz, and U. Wiedemann, *Ann. Rev. Nucl. Part. Sci.* **55**, 357 (2005), arXiv:nucl-ex/0505014.
- [7] L. Fabbietti, V. Mantovani Sarti, and O. Vazquez Doce, *Ann. Rev. Nucl. Part. Sci.* **71**, 377 (2021), arXiv:2012.09806 [nucl-ex].
- [8] J. Adamczewski-Musch *et al.* (HADES), *Phys. Rev. C* **94**, 025201 (2016), arXiv:1602.08880 [nucl-ex].
- [9] L. Adamczyk *et al.* (STAR), *Phys. Rev. Lett.* **114**, 022301 (2015), arXiv:1408.4360 [nucl-ex].
- [10] J. Adam *et al.* (STAR), *Phys. Lett. B* **790**, 490 (2019), arXiv:1808.02511 [hep-ex].
- [11] S. Acharya *et al.* (ALICE), *Phys. Lett. B* **774**, 64 (2017), arXiv:1705.04929 [nucl-ex].
- [12] S. Acharya *et al.* (ALICE), *Phys. Rev. C* **96**, 064613 (2017), arXiv:1709.01731 [nucl-ex].
- [13] S. Acharya *et al.* (ALICE), *Phys. Lett. B* **790**, 22 (2019), arXiv:1809.07899 [nucl-ex].
- [14] S. Acharya *et al.* (ALICE), *Phys. Lett. B* **833**, 137335 (2022), arXiv:2111.06611 [nucl-ex].
- [15] S. Acharya *et al.* (ALICE), *Phys. Rev. C* **103**, 055201 (2021), arXiv:2005.11124 [nucl-ex].
- [16] S. Acharya *et al.* (ALICE), *Phys. Rev. Lett.* **124**, 092301 (2020), arXiv:1905.13470 [nucl-ex].
- [17] S. Acharya *et al.* (ALICE), *Phys. Rev. C* **99**, 024001 (2019), arXiv:1805.12455 [nucl-ex].
- [18] S. Acharya *et al.* (ALICE), *Phys. Lett. B* **833**, 137272 (2022), arXiv:2104.04427 [nucl-ex].
- [19] S. Acharya *et al.* (ALICE), *Phys. Lett. B* **805**, 135419 (2020), arXiv:1910.14407 [nucl-ex].
- [20] S. Acharya *et al.* (ALICE), *Phys. Lett. B* **797**, 134822 (2019), arXiv:1905.07209 [nucl-ex].
- [21] S. Acharya *et al.* (ALICE), *Phys. Rev. Lett.* **123**, 112002 (2019), arXiv:1904.12198 [nucl-ex].
- [22] A. Collaboration *et al.* (ALICE), *Nature* **588**, 232 (2020), [Erratum: *Nature* 590, E13 (2021)], arXiv:2005.11495 [nucl-ex].
- [23] S. Acharya *et al.* (ALICE), *Phys. Lett. B* **813**, 136030 (2021), arXiv:2007.08315 [nucl-ex].
- [24] S. Acharya *et al.* (ALICE), *Phys. Rev. Lett.* **127**, 172301 (2021), arXiv:2105.05578 [nucl-ex].
- [25] S. Acharya *et al.* (ALICE), *Phys. Lett. B* **802**, 135223 (2020), arXiv:1903.06149 [nucl-ex].
- [26] S. Acharya *et al.* (ALICE), *Phys. Lett. B* **829**, 137060 (2022), arXiv:2105.05190 [nucl-ex].
- [27] S. Acharya *et al.* (ALICE), *Phys. Rev. D* **110**, 032004 (2024), arXiv:2401.13541 [nucl-ex].
- [28] S. Acharya and others [ALICE Collaboration], *Phys. Rev. X* **14**, 031051 (2024), arXiv:2308.16120 [nucl-ex].
- [29] STAR Collaboration, (2024), arXiv:2410.03436 [nucl-ex].
- [30] M. Stefaniak, *EPJ Web Conf.* **296**, 02001 (2024), arXiv:2401.12966 [nucl-ex].
- [31] R. Lednicky and V. L. Lyuboshits, *Yad. Fiz.* **35**, 1316 (1981).
- [32] R. Lednicky, *Phys. Part. Nucl.* **40**, 307 (2009), arXiv:nucl-th/0501065 [nucl-th].
- [33] J. Arvieux, *Nucl. Phys. A* **221**, 253 (1974).
- [34] M. Viviani, S. König, A. Kievsky, L. E. Marcucci, B. Singh, and O. Vazquez Doce, *Phys. Rev. C* **108**, 064002 (2023), arXiv:2306.02478 [nucl-th].

- [35] P. Danielewicz and G. F. Bertsch, Nucl. Phys. A **533**, 712 (1991).
- [36] Y. Oh, Z.-W. Lin, and C. M. Ko, Phys. Rev. C **80**, 064902 (2009), arXiv:0910.1977 [nucl-th].
- [37] D. Oliinychenko, C. Shen, and V. Koch (SMASH), Phys. Rev. C **103**, 034913 (2021), arXiv:2009.01915 [hep-ph].
- [38] J. Staudenmaier, D. Oliinychenko, J. M. Torres-Rincon, and H. Elfner (SMASH), Phys. Rev. C **104**, 034908 (2021), arXiv:2106.14287 [hep-ph].
- [39] A. Andronic, P. Braun-Munzinger, J. Stachel, and H. Stocker, Phys. Lett. B **697**, 203 (2011), arXiv:1010.2995 [nucl-th].
- [40] A. Andronic, P. Braun-Munzinger, K. Redlich, and J. Stachel, Nature **561**, 321 (2018), arXiv:1710.09425 [nucl-th].
- [41] B. K. Jennings, D. H. Boal, and J. C. Shillcock, Phys. Rev. C **33**, 1303 (1986).
- [42] P. Giannozzi, Numerical methods in quantum mechanics, <https://www.fisica.uniud.it/~giannozz/Corsi/MQ/LectureNotes/mq.pdf> (2020), University of Udine.
- [43] M. Macêdo-Lima and L. Madeira, Rev. Bras. Ens. Fis. **45**, e20230079 (2023), arXiv:2303.04591 [quant-ph].
- [44] C. J. Joachain, Quantum Collision Theory (North-Holland Publishing Company, Amsterdam, 1975).
- [45] F. Salvat and J. M. Fernandez-Varea, Computer Physics Communications **240**, 165 (2019).
- [46] W. T. H. Van Oers and K. W. Brockman, Nucl. Phys. A **92**, 561 (1967).
- [47] D. Eyre, A. C. Phillips, and F. Roig, Nucl. Phys. A **275**, 13 (1977).
- [48] E. Huttel, W. Arnold, H. Baumgart, H. Berg, and G. Clausnitzer, Nucl. Phys. A **406**, 443 (1983).
- [49] A. Kievsky, S. Rosati, W. Tornow, and M. Viviani, Nucl. Phys. A **607**, 402 (1996).
- [50] S. Pratt, T. Csorgo, and J. Zimanyi, Phys. Rev. C **42**, 2646 (1990).
- [51] W. Rzesza, M. Stefaniak, and S. Pratt, (2024), arXiv:2410.13983 [nucl-th].